Electromagnetic wave absorbing properties and hyperfine interactions of Fe-Cu-Nb-Si-B nanocomposites*

Han Man-Gui (韩满贵) [a)†], Guo Wei (郭韦) [a)], Wu Yan-Hui (吴燕辉) [a)], Liu Min (刘明) [b)], Magundappa L. Hadimani [c)], Deng Long-Jiang (邓龙江) [a)]

a) State Key Laboratory of Electronic Thin Films and Integrated Devices, University of Electronic Science and Technology of China, Chengdu, 610054, China.

b) Analytical and Testing Center, Sichuan University, Chengdu, 610064, China.

c) Department of Electrical and Computer Engineering, Iowa State University, Ames, IA 50011, USA.

Abstract

Fe-Cu-Nb-Si-B alloy nanocomposite containing two ferromagnetic phases (amorphous phase and nano phase phase) has been obtained by properly annealing the as-prepared alloys. High resolution transmission electron microscopy (HR-TEM) images have shown the coexistence of these two phases. It is found that Fe-Si nano grains are surrounded by the retained amorphous ferromagnetic phase. Mössbauer spectroscopy measurements have showed that the nano phase is the $D0_3$ type Fe-Si phase, and has been employed to find the atomic fractions of resonant ^{57}Fe atoms in these two phases. The microwave permittivity and permeability spectra of Fe-Cu-Nb-Si-B nanocomposite have been measured within 0.5- 10 GHz. Large relative microwave permeability values have been obtained. The results show that the absorber containing the nanocomposite flakes with a volume fraction of 28.59 % shows good microwave absorption properties. The reflection loss of the absorber is less than -10 dB within the frequency band of 1.93 – 3.20 GHz.

Key words: Mössbauer spectroscopy; magnetic permeability; nanocrystalline alloys

PACS: 33.45.+x, 75.50.Bb, 75.50.Tt.

---

*Project supported by the Research Fund for International Young Scientists of NSFC (No. 61250110544), National Natural Science Foundation of China (No. 61271039), the Scientific Foundation of Young Scientists in Sichuan (No.2012JQ0053), and the Program for New Century Excellent Talents in Universities (NCET-11-0060).

† Corresponding author. E-mail: mangui@gmail.com

This is a manuscript of an article from Chinese Physics B 23 (2014): 083301, doi: 10.1088/1674-1056/23/8/083301. Posted with permission.

1. Introduction

Electromagnetic properties (permittivity and permeability) of magnetic materials are important for the performances of many electronic devices operating at high frequency [1-2]. For example, the electromagnetic noise suppression in the field of electromagnetic compatibility (EMC) requires the materials having large magnetic losses or dielectric losses [3-4]. With increasing the operation frequencies of electronic devices upward to gigahertz (GHz), for instance, wireless local area network system (2.4 GHz) and active radio frequency identification label (2.45 GHz), it is imperative to develop materials which have good electromagnetic properties. It is well known that the spinel ferrites (Mn-Zn, Ni-Zn ferrites) or the hexagonal ferrites (Z-type or W-type) are the common magnetic oxides for the electromagnetic wave attenuation applications because of their high resistance and large magnetic losses arising from the natural resonance at radio frequencies (e.g. 1 MHz-300 MHz) or microwave frequencies (e.g. 500 MHz – 3 GHz) [5-7], respectively. However, in comparison with ferromagnetic alloys, these ferrites suffer from some severe shortcomings, such as worse temperature stability, lower Curie temperature, and smaller saturation magnetization (Ms) value [8]. These shortcomings hinder their applications at high frequency or in some harsh environment. The metallic ferromagnetic alloys do not have these shortcomings. But they suffer from the large eddy current effect at high frequency, especially at microwave frequency band. Some have tried to coat the ferromagnetic particles with non-magnetic layers [9-10]. Although the non-magnetic layer can reduce the eddy current effect, but the outer coating is non-ferromagnetic, which will not be helpful for attenuating incoming EM wave via the mechanism of magnetic losses. Therefore, here we speculate to develop a core-shell nanocomposite consisting of both ferromagnetic phases. It is well known that the amorphous ferromagnetic alloys have larger resistivity values than those of crystallized alloys [11]. If the amorphous phase forms a core shell on a nanocrystalline grain, the eddy current

This is a manuscript of an article from Chinese Physics B 23 (2014): 083301, doi: 10.1088/1674-1056/23/8/083301. Posted with permission.

effect should be able to be greatly alleviated for this nanocomposite. Fe-based nanocrystalline magnetic alloys are one of soft ferromagnetic materials with excellent properties, which are usually employed as the magnetic core materials with low magnetic loss at the frequency around 1 kHz – 1 MHz [12-14]. In this paper, we plan to develop a nanocomposite which have an amorphous phase and a nanocrystalline phase, and investigate their electromagnetic wave attenuation properties within the frequency range of 0.5 – 10 GHz.

2. Experimental details

$Fe_{77.8}Cu_{2.39}Nb_{3.33}Si_{16.28}B_{0.62}$ ribbons were manufactured with iron, copper, Fe-Nb alloy, and Fe-B alloy as the starting materials. These starting materials were melted in an induction furnace. The as-prepared ribbons were prepared by a rapid quench procedure called the melt-spinning technique. The differential scanning calorimeter (DSC) measurements have been carried out to find the phase transition temperatures (T_1 and T_2) with a heating rate of 5 °C/min. The as-prepared ribbons were then annealed to obtain the nanostructured phase under argon atmosphere. X-ray diffraction (XRD) measurements (Cu K_α radiation) were done to examine the phases of ribbons. High resolution-transmission electron microscopy (HR-TEM, Model: TECNAI-G^2 F20) was employed to investigate the nanostructures of annealed samples. HR-TEM images and selected area electron diffraction (SAED) were taken to study the size of nano grains and the formation of nano phases. Mössbauer spectroscopy experiments with the transmission geometry have been conducted for the annealed ribbons. The radiation source was with ^{57}Co radiation source in the rhodium (Rh) matrix. The velocity of radiation source is calibrated with a standard α-Fe foil. The Mössbauer spectra have been fitted using the software called WinNormos-for-Igors®. The annealed ribbons were milled into flakes for 10 hours by a planetary milling machine with ethanol as the milling dispersant. To measure the electromagnetic parameters (μ_r and ε_r), the flakes were mixed with the dispersant (paraffin) with a volume fraction of 28.59 % flakes to fabricate a toroidal shape measurement sample. The high frequency properties have been measured on a vector network analyzer (Agilent 8720 ET) within

the frequency range of 0.5 - 10 GHz based on the transmission/reflection approach by inserting the sample into a coaxial waveguide.

3. Results and discussions

In order to find the nanocrystallization temperature for the as-prepared ribbons, DSC measurements were taken, as shown in Fig. 1(a). Two exothermal peaks can be found. One is at 530 °C (called T_{x1}). The other one is at 672 °C (called T_{x2}). T_{x1} is called the primary crystallization temperature. T_{x2} is called the secondary crystallization temperature. In order to form nano scale grains, the as-prepared ribbons were annealed at 540 ^{0}C, which is between T_{x1} and T_{x2}. It is reported that nanoscale Fe(Si) grains can be formed [15]. XRD patterns shown in Fig. 1(b) indicate that the as-prepared ribbons are in the amorphous state. The ribbons after the heat treatment have been found to be partially nanocrystallized. XRD patterns of ribbons heat treated show that the nanocrystalline phase is α-Fe(Si). The HR-TEM images of annealed samples are shown in Fig. 2. The dark field image of TEM shows that the average grain size is about 14.38 nm, see Fig. 3(a). Fig. 2(b) shows the SAED pattern of the same sample, which manifests the coexistence of the amorphous phase and the nano phase. Multi diffraction rings have been observed, which indicate the formation of crystalline grains. The halo in the SAED pattern indicates the existence of the amorphous phase. HR-TEM images of these two phases are shown in Fig. 2(c) and (d). The spacing of (220) plane of Fe-Si nano grains is found to be about 2.0 Å, see Fig. 2(c). Crystal defects have also been found, as pointed out in the zones labeled “A” and “B” in Fig. 2(c). More importantly, it is evidenced in Fig. 2(d) that the nano grains are surrounded by the amorphous phase, such a core-shell nanostructure is what we intend to obtain and is believed helpful to alleviate the eddy current effect at GHz frequency. For Fe(Si) alloy, the occupancy of Fe and Si atoms in the crystal lattice can be random or ordered [16]. For an ordered Fe-Si alloy, the occupancy possibilities of Fe atom vary with the content of Si atoms. The Mössbauer spectroscopy technique is a powerful tool for studying such atomic occupancy differences. For instance, Fe atoms exist in both phases in the nanocomposite under study, it is easy and reliable to find the atomic fraction of Fe

This is a manuscript of an article from Chinese Physics B 23 (2014): 083301, doi: 10.1088/1674-1056/23/8/083301. Posted with permission.

atoms in the respective phase.

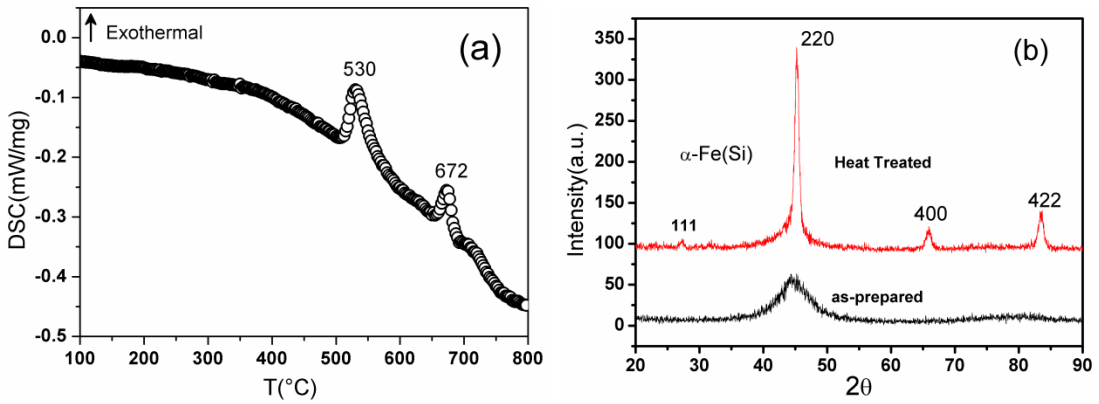

Fig. 1. (a) DSC curve; (b) XRD patterns.

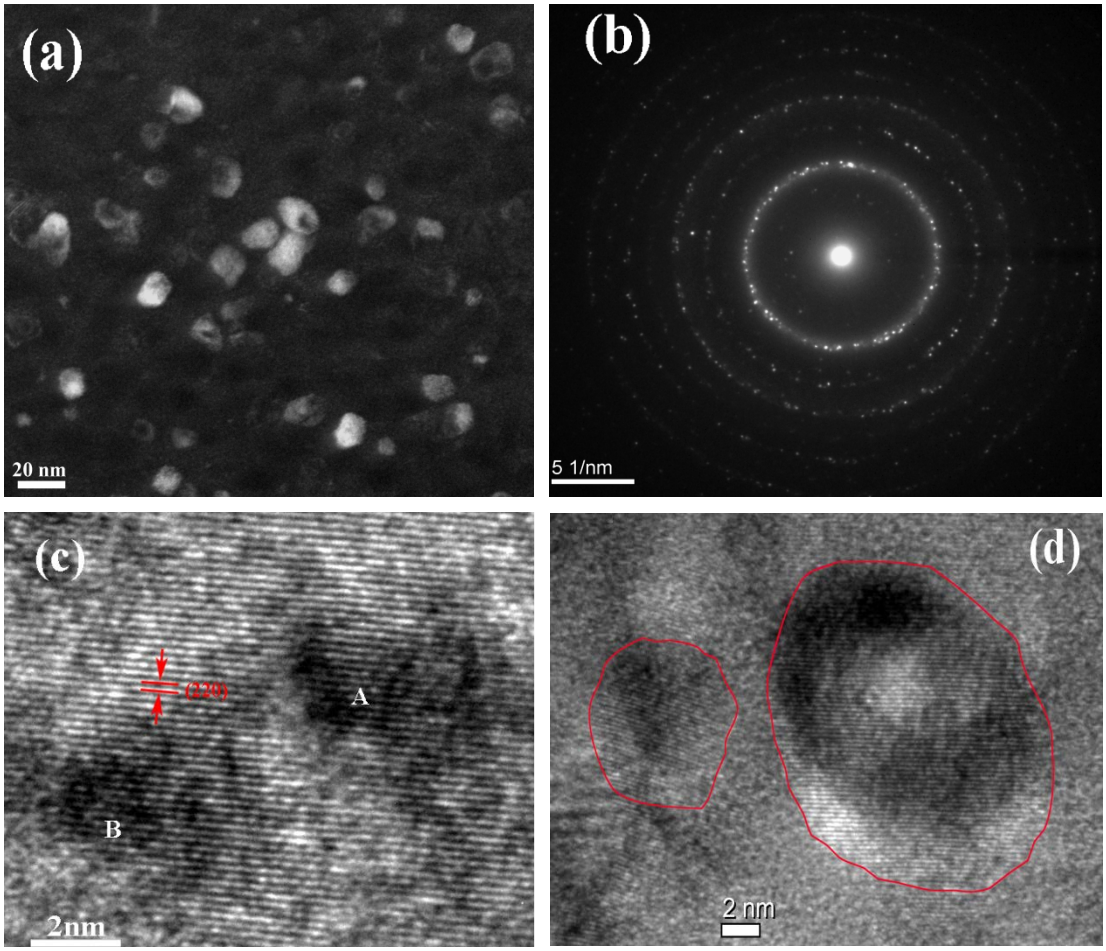

Fig. 2. TEM images. (a) dark field image; (b) SAED pattern; (c) and (d) high resolution images.

As we know that there are two ferromagnetic phases inside the alloy, one is the amorphous ferromagnetic phase, in which Fe atoms are distributed randomly. The other phase is $D0_3$ type Fe (Si) nano grains. The Mössbauer spectrum has been fitted by a combination of the component related to the distribution of hyperfine fields and

discrete spectral components with narrow lines originating from various Fe positions in the $D0_3$ type Fe-Si lattice. For our nanocomposite, four kinds of Fe atom environments can be classified according to Fig. 2(d) and the schematic presentation shown in Fig. 3(a). The first case (I) is that Fe atoms locate in Fe-Si nano grains, which can be represented by several discrete sextets. The second case (II) is that Fe atoms constitute the outer surface of a nano grain. The third case (III) is that Fe atoms situate in the interface between two nano grains or between the nano grain and the amorphous phase. The fourth case (IV) is that Fe atoms locate in the amorphous matrix with disordered atomic arrangement, which is not directly contacted with the nano grains. The second case (II) and the third case (III) are usually classified as the interface zone [17]. Fe atoms in this zone have the randomly disordered neighboring atoms. Therefore, a distribution hyperfine interactions model should be used to fit for Fe atoms located in the regions of II, III and IV.

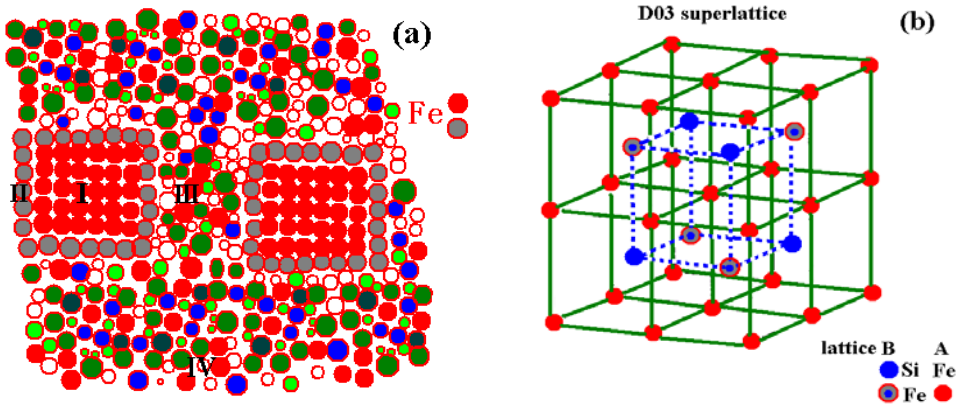

Fig. 3. Schematic representations of Fe environments in the nanocomposite and the D03 type Fe-Si superlattice.

The superlattice of Fe-Si is shown in Fig. 3(b), which consists of “A” lattice with sites occupied by Fe atoms, and “B” lattice with sites occupied by Fe and Si atoms. For each atom in “B” lattice, it has eight Fe atoms as its nearest neighbors. For each Fe atom in “A” lattice, it has a varying number of nearest-neighbor Fe or Si atoms depending on the Si concentration. The Mössbauer spectrum of Fe-based nanocrystalline alloy is shown in Fig. 4. Clearly, the fittings and the experimental data of Mössbauer agree very well, see Fig. 4(a). The fitting results show that the Mössbauer spectrum can be

This is a manuscript of an article from Chinese Physics B 23 (2014): 083301, doi: 10.1088/1674-1056/23/8/083301. Posted with permission.

resolved into 4 discrete sextets and one broad subspectrum labelled as "*am*.". Four resolved discrete sextets (labelled as 1 - 4 respectively) represent 4 possibilities of the nearest neighboring for ^{57}Fe atoms in the D03 type Fe-Si superlattice. The fitting results are shown in Table 1. The hyperfine magnetic fields (B_{hf}) we have obtained for these four discrete sextets are very close to those reported by others [16, 18]. "1" denotes the case of 8 Fe atoms as the nearest neighbor of a resonant ^{57}Fe atom, which can be simply marked as "8Fe0Si". In the same way, "2" denotes the case of "6Fe2Si". "3" denotes the case of "5Fe3Si". "4" denotes the case of "4Fe4Si". For each kind of neighboring occasions, the hyperfine magnetic field acting on the resonant ^{57}Fe atoms is given in Table 1. As for the ^{57}Fe atoms in the zone having random neighboring atoms (Fe, Cu, Nb, Si and B), the distribution of hyperfine interactions parameters (B_{hf} and isomer shift) are shown in Fig. 4(b). Clearly, the value of the hyperfine magnetic field mainly falls within the range of 10 – 40 Telsa. The distribution of hyperfine interactions originates from two regions, i.e. region II and III shown in Fig. 3(a). The relative areas for each sextet reveal the possibilities of each surrounding, which are also given in Table 1. The relative atomic fractions of Fe atoms in the amorphous phase and nano phase are 42.635 % and 57.365% respectively, as indicated in Table 1.

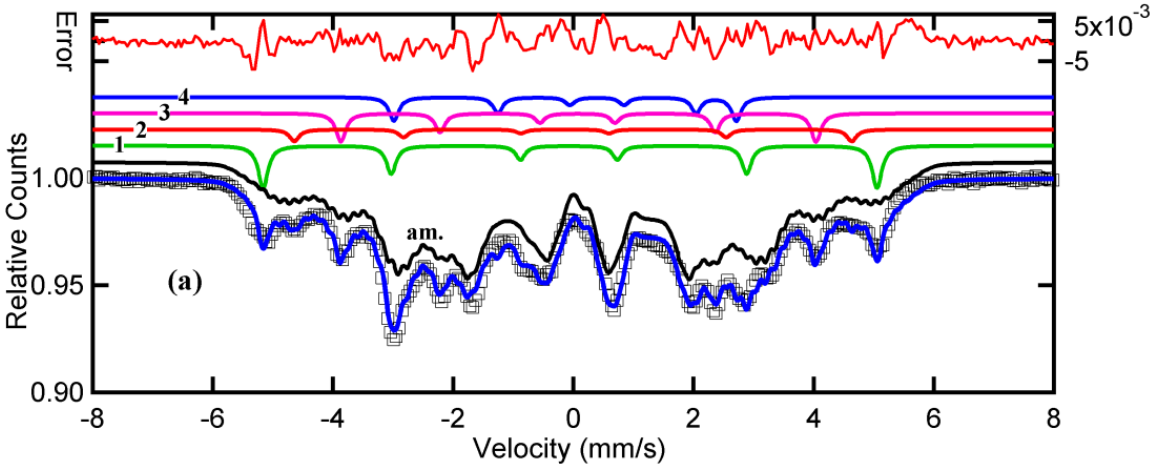

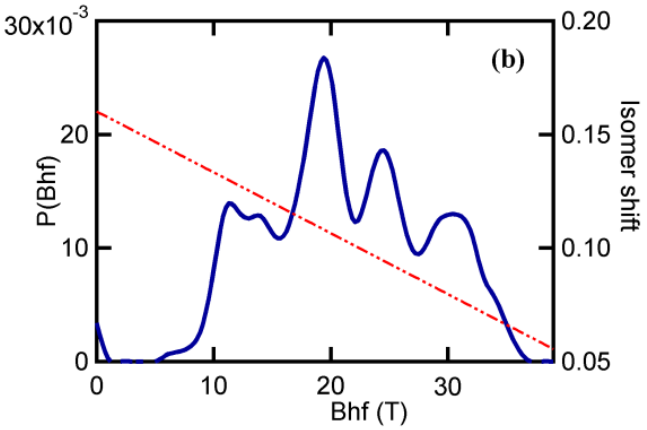

Fig.4. Mössbauer spectra of Fe-Cu-Nb-Si-B nanocomposites.

Table: Fitting results of Mössbauer spectrum

	Amorphous	S1	S2	S3	S4
B_{hf} (Tesla)	21.149	31.684	28.776	24.525	17.677
Percentage (%)	42.635	18.511	9.771	15.207	13.877

The electromagnetic properties of Fe-Cu-Nb-Si-B nanocomposites are shown in Fig. 5. The dependence of relative complex permittivity on frequency is shown in Fig. 5(a). It is found that the variation of permittivity is not obvious within the frequency range of 0.5 - 4 GHz. Besides, the high frequency dielectric loss is insignificant within this frequency range. However, it is observed that the complex permeability significantly varies with the frequency. A wide magnetic loss peak (i.e. $\mu'' \sim f$) are obviously seen in Fig. 5(b). Once the dependences of permittivity and permeability on frequency have been measured, the electromagnetic wave (EM) absorption of an absorber containing these ferromagnetic flakes with the reported nanocomposite features can be evaluated by the following equations. The properties of EM absorption are characterized by the reflection loss (R. L.) [19-21].

$$Z_{in} = Z_0\sqrt{\mu_r/\varepsilon_r}\, tanh\left\{j\left(\frac{2\pi f t}{c}\right)\sqrt{\mu_r\varepsilon_r}\right\} \qquad (1)$$

$$R.L. = 20log|(Z_{in} - Z_0)/(Z_{in} + Z_0)| \qquad (2)$$

, where "Z_{in}" is the input impedance of the absorber, "Z_0" is the impedance of the free space, "t "is the thickness of an absorber, and "c" is the speed of light. The results in Fig. 6 show that when the thickness of the absorber is 4 mm, good electromagnetic

wave attenuation can be achieved. Within the frequency range of 1.93 – 3.20 GHz, The value of R. L. is less than -10 dB.

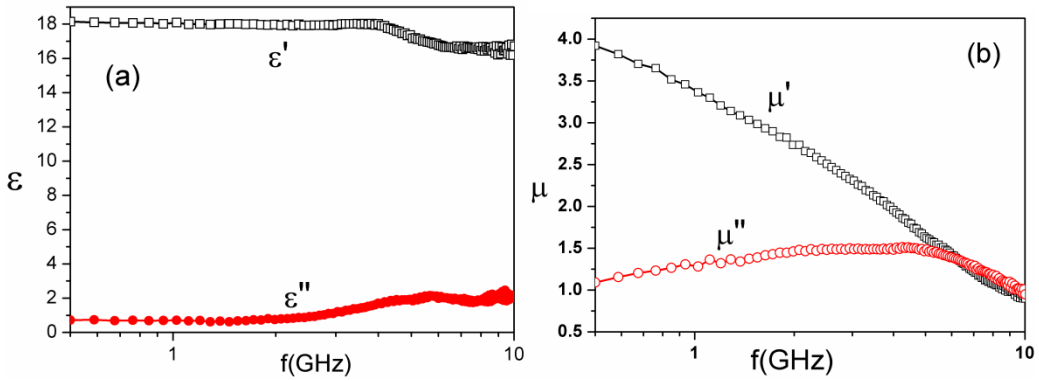

Fig. 5. Microwave permittivity and permeability spectra of Fe-based nanocomposites

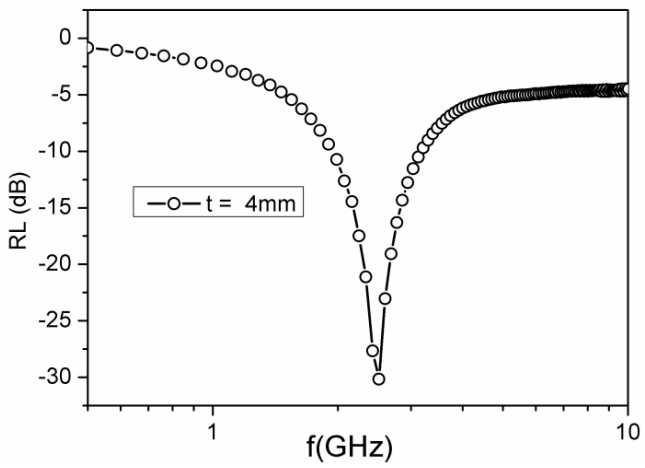

Fig.6. Microwave absorption properties of the Fe-based nanocomposite.

4. Conclusions

The as-prepared Fe-Cu-Nb-Si-B alloys are found to be amorphous. Nanocomposite containing core-shell nanostructures has been obtained by heat treatments. The cores are Fe-Si nano grains. The shell is amorphous phase. Both the core and shell are ferromagnetic, which have been verified by Mössbauer measurements. HR-TEM results show the average grain size of nano phase is about 14.38 nm. Mössbauer spectroscopy results show that the nano grains are Fe-Si alloy with the $D0_3$ type superlattice structure with an atomic fraction of 57.365 % for Fe atoms. Large microwave permeability values have been found in the nanocomposites. Within the frequency range of 1.93 – 3.20 GHz, the absorber containing the flakes with the nanostructures shows good electromagnetic wave attenuation properties when the

thickness of an absorber is 4 mm.

References

[1] Marian K. Kazimierczuk, *High-frequency magnetic components*, John Wiley & Sons, Ltd, (2009).

[2] Li S., Liu M., Lou J., Xing X., Wu J., Hu Y., Cai X., Xu F., Sun N. X., Duh Jenq-Gong, *J. Nanosci. Nanotech.*, **13** (2013)1091-1094.

[3]Han Y., Cheung G., Li A., Sullivan C. R., and David J. P., *IEEE Trans. Power Electr.* **27** (2012) 425-435.

[4] Abbas S. M., Chandra M., Verma A., Chatterjee R., Goel T. C., *Composites Part A*，**37** (2006)2148.

[5] Nakamura T., *J. Appl. Phys.* **88** (2000) 348.

[6] Korolev K. A., McCloy J. S., and Afsar M. N., *J. Appl. Phys.* **111**(2012) 07E113-1.

[7] Nakamura T., Hankui E., *J. Magn. Magn. Mater.* **257** (2003)158.

[8] Goldman Alex, Modern ferrites Technology (2nd edition), Springer, 2006.

[9] Yan Longgang, Wang Jianbo, Han Xianghua, Ren Yong, Liu Qingfang and Li Fashen, *Nanotech.*, **21** (2010) 095708.

[10]Yang Xin-Chun, Liu Rui-Jiang, Shen Xiang-Qian, Song Fu-Zhan, Jing Mao-Xiang and Meng Xian-Feng, *Chin. Phys. B*, **22** (2013) 058101.

[11] Chiriac H., Ovari T., *Prog. Mater. Sci.* **40**(1996)333.

[12] Varga L. K. and Kovacs G., *IEEE Trans. Magn.* **48** (2012)1360.

[13] Kuzmann E., Stichleutner S., Sapi A., Klencsar Z., Oshtrakh M. I., Semionkin V. A., Kubuki S., Homonnay Z., Varga L. K., *Hyperfine Interact.*, **219** (2013) 63.

[14] Füzerová J., Füzer J., Kollár P., Bureš R., Fáberová M., *J. Magn. Magn. Mater.*, **345** (2013)77.

[15] Michael E. McHenry, Matthew A. Willard, David E. Laughlin, *Prog. Mater. Sci.*, **44** (1999) 291.

[16] Stearns M. B., *Phys. Rev.*, **129** (1963) 1136.

[17] Miglierini M., Greneche J. M., *J. Phys.: Condens. Matter.*, **9**(1997) 2303.

[18] Kopcewicz M., Chapter 5 “Mössbauer spectroscopy characterization of soft magnetic nanocrystalline alloys, pg. 151 – 265. *Handbook of Advanced Magnetic Material* (II), Tsinghua

University Press, 2005.

[19] Naito Y., Suetake K., *IEEE Trans. Microwave Theory Tech.*, **19** (1971) 65.

[20] Han M., Liang D., Deng L., *Appl. Phys. Lett.*, **99** (2011)082503.

[21]Lu H. P., Han M.G., Cai L., Deng L.J., *Chin. Phys. B,* **20** (2011)060701.